PHYSICAL REVIEW LETTERS

Acceptor Levels in *p*-Type Cu$_2$O: Rationalizing Theory and Experiment

David O. Scanlon,[*] Benjamin J. Morgan, and Graeme W. Watson[†]

School of Chemistry, Trinity College Dublin, Dublin 2, Ireland

Aron Walsh

Department of Chemistry, University College London, 20 Gordon Street, London, WC1H 0AJ, United Kingdom

Understanding conduction in Cu$_2$O is vital to the optimization of Cu-based *p*-type transparent conducting oxides. Using a screened hybrid–density-functional approach we have investigated the formation of *p*-type defects in Cu$_2$O giving rise to single-particle levels that are deep in the band gap, consistent with experimentally observed activated, polaronic conduction. Our calculated transition levels for simple and split copper vacancies explain the source of the two distinct hole states seen in DLTS experiments. The necessity of techniques that go beyond the present generalized-gradient- and local-density-approximation techniques for accurately describing *p*-type defects in Cu(I)-based oxides is discussed.

Cuprous oxide (Cu$_2$O) is a prototypical *p*-type conducting oxide with applications in photovoltaics, dilute magnetic semiconductors, low cost solar cells, gas sensors, and catalysis [1]. Cu$_2$O is also the parent compound of many *p*-type transparent conducting oxides (TCOs) such as Cu*M*O$_2$ delafossites (*M* = Al, Cr, B, In, Ga, etc.) [2] and SrCu$_2$O$_2$ [3], which are thought to retain the valence-band features and conduction mechanisms of Cu$_2$O [4]. The design and fabrication of high figure of merit *p*-type TCOs is a major goal for materials scientists, as this will enable "invisible electronics" based on transparent *p*-*n* junctions. An understanding of the defect chemistry and conduction properties of Cu$_2$O is therefore vital to the optimization of these technologically important Cu(I)-based *p*-type TCOs.

The conduction behavior Cu$_2$O is not that of classical semiconductors, but occurs by a *polaronic* hopping mechanism [5–7], demonstrated by Arrhenius-like temperature dependence [8–11]. Conduction arises due to oxygen excess exhibited as copper vacancies, V_{Cu}, or oxygen interstitials, O$_i$. These defects introduce hole states above the valence-band maximum (VBM), due to the oxidation of Cu(I) to Cu(II) [12].

In Cu$_2$O hole states (acceptor levels) have been reported in experiments in the range 0.12–0.70 eV above the VBM [13–19]. The exact nature of the defects that give rise to these states has, however, been a source of controversy [13–23]. Deep level transient spectroscopy (DLTS) has shown the presence of hole traps 0.45–0.55 eV above the VBM [13–15], attributed to structural anomalies, such as CuO islands. A recent DLTS study, with a broader temperature range of 100 to 350 K, reported two trap levels [19]. A hole trap at 0.45 eV above the VBM, as identified previously, was attributed to V_{Cu}, and a new trap level at 0.25 eV was tentatively assigned to a Cu divacancy.

p-type defects in Cu$_2$O have received limited attention in theoretical studies [22–25]. Wright *et al.* studied the energetics of V_{Cu} in Cu$_2$O using density-functional theory (DFT) and the local density approximation (LDA) [25], and found that a "simple" copper vacancy, V_{Cu}, in which one Cu is removed leaving two three-coordinate oxygens, is less stable than a "split" vacancy geometry, V_{Cu}^{split}, where one remaining Cu moves toward the vacancy site, to achieve tetrahedral coordination. DFT-generalized gradient approximation (GGA) and DFT-GGA + *U* techniques were used by Nolan and Elliott, who reported that V_{Cu} was 0.06 eV more favorable than V_{Cu}^{split} [22]. Delocalized states were reported for each vacancy with both methods, with defect bands crossing the Fermi level resulting in a notionally metallic system.

Raebiger *et al.* studied intrinsic defects in Cu$_2$O using GGA with the addition of *a posteriori* corrections to correct defect energies and transition levels [23]. They found V_{Cu} to be the most favored defect, and hence suggested it as the most likely source of *p*-type charge carriers. The calculated $(0/-1)$ transition level for V_{Cu} was ∼0.28 eV, which the authors equated to the trap at 0.25 eV reported in the DLTS study of Paul *et al.* [19]. These calculated levels, however, included a rigid shift of 0.32 eV applied to the VBM of the GGA calculation, derived from a separate reference GGA + *U* bulk calculation, which can introduce inaccuracies to level positions [26].

For all previous GGA calculations, the single-particle levels (SPL, or raw eigenvalues) of the hole states for V_{Cu} were resonant in the VB, leading to predictions of metallic conductivity [22–24]. This is inconsistent with the activated, polaronic, experimental behavior, however, and suggests post-LDA and -GGA methods are necessary for modeling *p*-type defects in Cu$_2$O.

In this Letter we present a hybrid-DFT examination of the single-particle levels and transition levels of acceptor-

096405-1

level–forming defects in Cu_2O. Hybrid-DFT incorporates a proportion of nonlocal exact Hartree-Fock exchange that acts to correct the self-interaction error (SIE) inherent to GGA and LDA functionals [27], and which is responsible for the delocalized nature of the semimetallic hole states obtained with GGA [22–24]. We report for the first time distinct single-particle levels above the VBM for *all* p-type defects investigated; a finding congruous with the polaronic behavior expected from experiment. We demonstrate the most favored defect is V_{Cu}^{split}, with V_{Cu} also expected to be present in experimental samples. The transition levels for these two favored defects explain the appearance of the two distinct hole traps seen in DLTS experiments. Thus the use of methods beyond GGA and LDA are shown to successfully model p-type defects in Cu_2O. It is expected that these results will serve as a guide to understanding defect physics and conductivity in Cu(I)-based TCOs.

Method.—As defects in Cu_2O are polaronic [6,7], we utilize a hybrid-DFT approach to counteract the problems associated with the SIE inherent to standard GGA and LDA functionals [27]. Post-LDA and -GGA methods have been shown to be necessary for a number of correlated materials where polaronic defects have proved problematic for standard functionals due to the SIE [28,29]. Hybrid-DFT functionals have recently become more computationally tractable, and have become invaluable in solid state simulations, often providing better structural data and more accurate band gaps [30–32]. We used the screened HSE hybrid density functional [33], as implemented in the VASP code [34]. The value of exact nonlocal exchange, α, was 27.5%, which gives a band gap of 2.12 eV, in excellent agreement with the experimentally measured band gap of 2.17 eV [35]. Interactions between the cores (Cu:[Ar] and O:[He]) and the valence electrons were described using the PAW method [36]. A plane wave cutoff of 400 eV and k-point sampling of $4 \times 4 \times 4$ for stoichiometric Cu_2O were used, and the structure was deemed to be converged when the forces on all the atoms were less than 0.01 eV $Å^{-1}$. Defects were calculated in a cubic $2 \times 2 \times 2$ (48 atom) supercell, and all calculations were spin polarized.

The formation enthalpy of a defect with charge state q is

$$\Delta H_f(D, q) = (E^{D,q} - E^H) + \sum_i n_i(E_i + \mu_i) + qE_F, \quad (1)$$

where $E_F = \Delta E_F + \epsilon_{VBM}^H + \Delta v(D)$.   (2)

E^H is the total energy of the stoichiometric host supercell and $E^{D,q}$ is the total energy of the defective cell. Elemental reference energies, E_i, were obtained from calculations on the constituent elements in their standard states, i.e., $O_{2(g)}$ and $Cu_{(s)}$. n is the number of atoms atom formally added to an external reservoir. The chemical potentials, μ_i, reflect the specific equilibrium growth conditions, within the global constraint of the calculated enthalpy of the host, in this instance Cu_2O: $2\mu_{Cu} + \mu_O = \Delta H_f^{Cu_2O} = -1.59$ eV.

The lower limit for μ_O, which characterizes a Cu-rich–O-poor environment, is determined by the formation of metallic Cu: $\Delta\mu_{Cu} = 0$ eV; $\Delta\mu_O = -1.59$ eV. The upper bound of μ_O (Cu-poor–O-rich) is limited by CuO formation: $\mu_{Cu} + \mu_O \leq \Delta H_f^{CuO} = -1.46$ eV, which yields $\Delta\mu_{Cu} = -0.13$ eV; $\Delta\mu_O = -1.34$ eV. E_F ranges from the VBM ($E_F = 0$ eV) to the CBM ($E_F = 2.17$ eV). ϵ_{VBM}^H is the VBM eigenvalue of the host bulk and $\Delta v(D)$ is the core-level alignment of the defective and bulk cells, given by $\Delta v(D) = \epsilon_{core,1s}^{far}(D, q) - \epsilon_{core,1s}^H$, where $\epsilon_{core,1s}^{far}(D, q)$ is the O 1s core energy level of the furthest O atom from the defect location, and $\epsilon_{core,1s}^H$ is the O 1s core energy level for the host supercell. The thermodynamic ionization (transition) levels of a given defect, $\epsilon_D(q/q')$, are equal to the Fermi-level for which charge states q and q' have equal energy:

$$\epsilon_D(q/q') = \frac{\Delta H^f(D, q) - \Delta H^f(D, q')}{q' - q}. \quad (3)$$

These transition levels can be compared directly to the levels reported in experiments where the final charge state can relax to its equilibrium configuration after the transition, of which DLTS is particularly appropriate [37].

Localization versus delocalization of hole states.—All the defects display acceptor SPL deep in the band gap (Fig. 1 and Table I), as expected for a polaronic system, and thus in agreement with experimental data. This is in contrast to the delocalized defect states predicted by previous calculations performed with standard GGA functionals [22–24]. Raebiger *et al.* proposed p-type conductivity in Cu_2O is due to holes produced by V_{Cu}, which reside in "delocalized, valence-band-like perturbed-host states" and not split off "defect-localized" states [23]. Such a description is, however, at variance with the experimentally known activated, polaronic, hopping mechanism [6,7]. It is noteworthy that the typical resistivity of Cu_2O is 35 Ω cm [38], which is considerably higher than the resistivities expected for classical band-conducting semiconductors, but which is in keeping with our calculated SPL being deep in the band gap.

Analysis of the hole charge densities associated with these defects reveals distinct *polaronic centers*. The hole
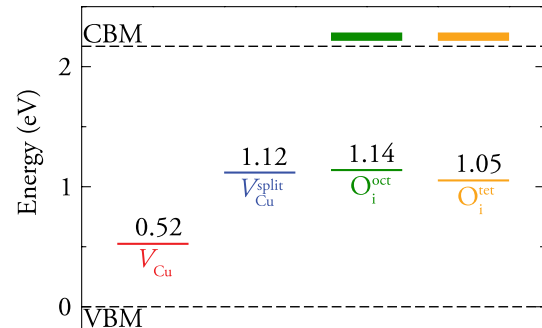

FIG. 1 (color online). HSE single-particle level offsets from the VBM of V_{Cu}, V_{Cu}^{split}, O_i^{oct}, and O_i^{tet}.

TABLE I. Formation energies $\Delta H_f(D, 0)$ in Cu-rich–O-poor conditions, single-particle (eigenvalue) levels for the hole states, and acceptor transition levels, $\epsilon_D(0/-1)$ for the four calculated p-type defects in Cu₂O.

	$\Delta H_f(D)$ (eV)				Single-particle level (eV)				$\epsilon_D(0/-1)$ (eV)			
	V_{Cu}	V_{Cu}^{split}	O_i^{oct}	O_i^{tet}	V_{Cu}	V_{Cu}^{split}	O_i^{oct}	O_i^{tet}	V_{Cu}	V_{Cu}^{split}	O_i^{oct}	O_i^{tet}
This work	1.15	1.14	1.94	1.87	0.52	1.11	1.13	1.05	0.23	0.47	1.08	1.27
GGA [22]	0.41	0.47	⋯	⋯	0.00	⋯	⋯	⋯	⋯	⋯	⋯	⋯
GGA* [23]	0.70	1.00	1.80	1.30	0.00	⋯	⋯	⋯	0.28	0.29	0.66	0.78
GGA [24]	0.47	0.78	1.90	1.47	0.00	⋯	⋯	⋯	0.18	0.20	0.45	0.65

state for V_{Cu} is localized on the six copper ions bonded to the two three-coordinate oxygens, with some hole density residing on the two oxygens themselves. The V_{Cu}^{split} hole state is strongly localized on the copper that moves towards the vacancy, and has Cu d character, with some mixing with the $2p$ states on the four oxygens tetrahedrally coordinated around the central Cu; Fig. 2. The hole states for both O_i^{oct} and O_i^{tet} are localized mainly on the interstitial oxygen and the surrounding Cu ions. In all cases, the defect centers are localized polarons, in contrast to the delocalized hole states predicted by GGA calculations [22,23].

Defect energetics and transition levels.—Figure 3(a) and Table I give the calculated formation enthalpies of all the intrinsic p-type defects calculated for Cu₂O in different charge states for Cu-rich–O-poor conditions. Under Cu-rich conditions V_{Cu}^{split} has the lowest formation enthalpy of all the defects investigated, with the formation energy of V_{Cu} only 0.01 eV greater. This agrees with the LDA study of Wright *et al.* who found V_{Cu}^{split} to be most stable [25], and is at variance with all previous GGA calculations [22–24]. Formation enthalpies for both V_{Cu} and O_i are lowered under Cu-poor–O-rich conditions [Fig. 3(b)], with the trend in formation energies unchanged. Copper vacancies (V_{Cu} and V_{Cu}^{split}) have the lowest formation energies under

all conditions and are therefore the likely cause of hole carriers in Cu₂O.

The calculated $\epsilon(0/-)$ transition levels for V_{split} (0.47 eV) and for V_{Cu} (0.22 eV) are in excellent agreement with the trap levels reported in the DLTS study of Paul *et al.* [19] at 0.45 and 0.25 eV above the VBM, and with those in a more recent DLTS study of Cu₂O by the same authors that finds trap levels at 0.5 and 0.21 eV [39]. That two distinct hole traps are found in DLTS spectra is explained by the similar formation energies of the V_{split} and V_{Cu} and their differing transition levels. The calculated transition levels of the oxygen interstitials are ultra deep, with the $\epsilon(0/-)$ transition levels at 1.08 and 1.28 eV, and the $\epsilon(-/-2)$ transition levels 1.36 and 1.98 eV above the VBM for the O_i^{oct} and O_i^{tet} respectively. The suggestion by Raebiger *et al.* that O_i could be the source of the deeper trap levels (0.45 eV) is shown to be an artifact of the inability of GGA to describe the polaronic states of Cu₂O properly [23], and we conclude that oxygen interstitials do not contribute to p-type conductivity in Cu₂O, as defect formation is energetically disfavored and the transition levels are too deep.

Conclusions.—The results presented assign the two trap levels reported in DLTS studies of Cu₂O to the $\epsilon(0/-)$ transition levels of V_{Cu} and V_{split}. The polaronic nature of Cu₂O is correctly described for the first time in a DFT
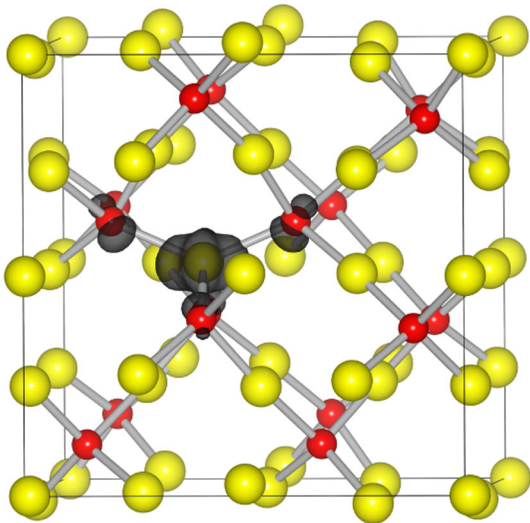

FIG. 2 (color online).   HSE ($\alpha = 27.5\%$) hole density for V_{Cu}^{split} in Cu₂O. The red and yellow spheres denote O and Cu, respectively. The blue isosurface is shown at $0.05e$ Å^{-3}.
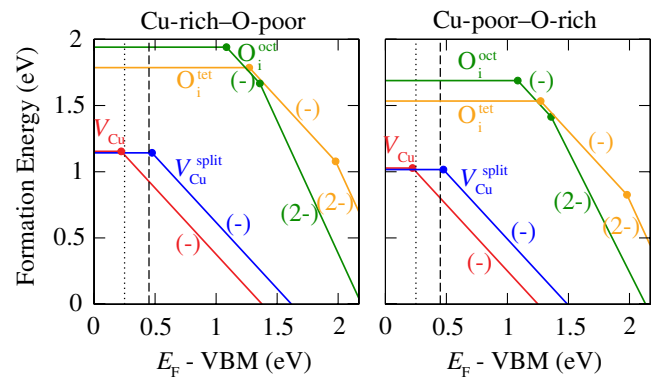

FIG. 3 (color online).   Formation energies for intrinsic p-type defects in Cu₂O in (a) Cu-rich–O-poor conditions and (b) Cu-poor–O-rich conditions. The solid dots denote the transition levels $\epsilon(q/q')$. The dotted and the dashed lines indicate the position of traps A and B from the DLTS study of Paul *et al.* [19].

study, with relatively deep single-particle levels found for *all p*-type defects. This can help explain the poor performance of Cu_2O thin-film solar cells; these deep acceptor levels will pin the Fermi level in the band gap, resulting in the extremely low open circuit voltages of 0.0–0.4 eV observed [40,41].

Hybrid-DFT reveals a qualitatively different description for defect properties in Cu_2O, which fully explains the nature of the experimentally observed hole traps. This confirms that LDA and GGA functionals are inappropriate for modeling this system. Furthermore, since conduction in Cu-based TCOs is known to be similarly polaronic [42–44], it is likely that hybrid functionals will be necessary for modeling these materials. This new understanding of localized behavior in these Cu(I)-based materials should serve as a guide to theoreticians and experimentalists alike who treat Cu(I)-based oxide materials as classical semiconductors.

---

*scanloda@tcd.ie

†watsong@tcd.ie

[1] S. Kale, S. Ogale, S. Shinde, M. Sahasrabuddhe, V. Kulkarni, R. Greene, and T. Venkatesan, Appl. Phys. Lett. **82**, 2100 (2003).

[2] X. Nie, S.-H. Wei, and S. B. Zhang, Phys. Rev. Lett. **88**, 066405 (2002).

[3] A. Kudo, H. Yanagi, H. Hosono, and H. Kawazoe, Appl. Phys. Lett. **73**, 220 (1998).

[4] A. N. Banerjee and K. K. Chattopadhyay, Prog. Cryst. Growth Char. Mater. **50**, 52 (2005).

[5] J. W. Hodby, T. E. Jenkins, C. Schwab, H. Tamura, and D. Trivich, J. Phys. C **9**, 1429 (1976).

[6] J. H. Park and K. Natesan, Oxid. Met. **39**, 411 (1993).

[7] A. Bose, S. Basu, S. Banerjee, and D. Chakravorty, J. Appl. Phys. **98**, 074307 (2005).

[8] R. S. Toth, R. Kilkson, and D. Trivich, Phys. Rev. **122**, 482 (1961).

[9] J. Maluenda, R. Farhi, and G. Petot-Ervas, J. Phys. Chem. Solids **42**, 911 (1981).

[10] L. C. Bourne, P. Y. Yu, A. Zettl, and M. L. Cohen, Phys. Rev. B **40**, 10973 (1989).

[11] T. Mahalingham, J. Chitra, S. Rajendran, and P. Sebastian, Semicond. Sci. Technol. **17**, 565 (2002).

[12] J. P. Hu, D. J. Payne, R. G. Egdell, P. A. Glans, T. Learmonth, K. E. Smith, J. Guo, and N. M. Harrison, Phys. Rev. B **77**, 155115 (2008).

[13] L. Papadimitiriou, C. A. Dimitriadis, and L. Dozsa, Solid State Electron. **31**, 1477 (1988).

[14] L. Papadimitiriou, Solid State Commun. **71**, 181 (1989).

[15] L. Papadimitiriou, Solid State Electron. **36**, 431 (1993).

[16] A. E. Rakhshani, Y. Makdisi, and X. Mathew, Thin Solid Films **288**, 69 (1996).

[17] R. Garuthara and W. Siripala, J. Lumin. **121**, 173 (2006).

[18] N. Kikuchi, K. Tonooka, and E. Kusano, Vacuum **80**, 756 (2006).

[19] G. K. Paul, Y. Nawa, H. Sato, T. Sakurai, and K. Akimoto, Appl. Phys. Lett. **88**, 141901 (2006).

[20] A. E. Rakhshani, J. Appl. Phys. **69**, 2365 (1991).

[21] J. Bloem, Phillips Research Reports **13**, 167 (1958).

[22] M. Nolan and S. D. Elliot, Phys. Chem. Chem. Phys. **8**, 5350 (2006).

[23] H. Raebiger, S. Lany, and A. Zunger, Phys. Rev. B **76**, 045209 (2007).

[24] A. Soon, X. Y. Cui, B. Delley, S.-H. Wei, and C. Stampfl, Phys. Rev. B **79**, 035205 (2009).

[25] A. F. Wright and J. S. Nelson, J. Appl. Phys. **92**, 5849 (2002).

[26] D. O. Scanlon, B. J. Morgan, and G. W. Watson, J. Chem. Phys. (to be published).

[27] P. Mori-Sánchez, A. J. Cohen, and W. Yang, Phys. Rev. Lett. **100**, 146401 (2008).

[28] B. J. Morgan and G. W. Watson, Surf. Sci. **601**, 5034 (2007).

[29] D. O. Scanlon, A. Walsh, B. J. Morgan, and G. W. Watson, J. Phys. Chem. C **112**, 9903 (2008).

[30] J. L. F. Da Silva, M. V. Ganduglia-Pirovano, J. Sauer, V. Bayer, and G. Kresse, Phys. Rev. B **75**, 045121 (2007).

[31] A. Walsh, J. L. F. Da Silva, Y. Yan, M. M. Al-Jassim, and S. H. Wei, Phys. Rev. B **79**, 073105 (2009).

[32] J. Paier, R. Asahi, A. Nagoya, and G. Kresse, Phys. Rev. B **79**, 115126 (2009).

[33] S. Heyd, G. E. Scuseria, and M. Ernzerhof, J. Chem. Phys. **118**, 8207 (2003).

[34] J. Paier, M. Marsman, K. Hummer, G. Kresse, I. C. Gerber, and J. G. Ángyán, J. Chem. Phys. **124**, 154709 (2006).

[35] A. Önsten, M. Månsson, T. Claesson, T. Muro, T. Matsushita, T. Nakamura, T. Kinoshita, U. O. Karlsson, and O. Tjernberg, Phys. Rev. B **76**, 115127 (2007).

[36] G. Kresse and J. Furthmuller, Comput. Mater. Sci. **6**, 15 (1996).

[37] R. M. Nieminen, *Theory of Defects in Semiconductors*, Topics in Applied Physics (Springer, Berlin, 2007).

[38] O. M. Madelung, *Semiconductors: Data Handbook* (Springer, Berlin, 2004).

[39] G. K. Paul, R. Ghosh, K. Bera, S. Bandyopadhyay, T. Sakurai, and K. Akimoto, Chem. Phys. Lett. **463**, 117 (2008).

[40] W. M. Sears and E. Fortin, Solar Energy Mater. Sol. Cells **10**, 93 (1984).

[41] J. A. Assimos and D. Trivich, J. Appl. Phys. **44**, 1687 (1973).

[42] F. A. Benko and F. P. Koffyberg, J. Phys. Chem. Solids **48**, 431 (1987).

[43] B. J. Ingram, G. B. Gonzalez, T. O. Mason, D. Y. Shahriari, A. Barnabe, D. Ko, and K. R. Poeppelmeier, Chem. Mater. **16**, 5616 (2004).

[44] B. J. Ingram, B. J. Harder, N. W. Hrabe, T. A. Mason, and K. R. Poeppelmeier, Chem. Mater. **16**, 5623 (2004).